Cite this article as: Martinón-Torres, M. and Uribe-Villegas, M.A. 2015. The prehistoric individual, connoisseurship and archaeological science: the Muisca goldwork of Colombia. *Journal of Archaeological Science* 63: 136-166. DOI: http://dx.doi.org/10.1016/j.jas.2015.08.014

Supplementary material

S1. Supplementary information on pXRF analyses

Three different pXRF instruments were employed, although all of them from the same manufacturer and with comparable evaluation settings. Table S1 details the specific analytical protocols for each of them. The main difference is that analyses with pXRF2011 were performed with an uncollimated beam of approximately 10 mm in diameter, whereas pXRF2012 and pXRF2013 were carried out with a 3mm collimator and higher beam current (Table S1). All instruments showed acceptable precision, with coefficients of variation for repeat analyses typically ≤2% for major elements, within and between days. Custom-made reference alloys were analysed with the pXRF2013 to confirm the accuracy of this instrument (Table S2), and values from this were therefore used as benchmarks to assess the reliability of pXRF2011 and pXRF2012 through comparisons of sets of artefacts that were analysed by two different instruments. These comparisons show that relative differences among instruments were very low for gold (δ relative ≤2%), whereas pXRF 2011 systematically overestimated silver levels by 6-8% relative. We therefore applied 0.94x as a correction factor for pXRF2011 silver values, which brought δ relative scores to ≤2%. The divergence between datasets is slightly more problematic for copper, particularly when this analyte is in concentrations ≤2%, but no correction factors were applied to this element as the differences were found to be less systematic (Tables S3 and S4).

Figure S1 shows comparisons between results for pXRF2011 vs pXRF 2012, and pXRF2012 vs pXRF2013, respectively. The scatterplots are based on average values from at least three measurements of the same artefacts by each of the instruments.

All the analyses were performed on unprepared surfaces. Based on our experience on ideal samples such as reference materials, pXRF can reliably identify and quantify heavy elements in concentrations down to 0.1% under this set up. However, sampling uncertainty is increased in our case because of analytical surfaces that are neither clean nor perfectly flat: increased background noise may result in false peak identifications, or even positively identified minor elements may just reflect surface enrichment from mild corrosion or burial environment. Thus, although some analyses inconsistently yielded small (<0.5%) concentrations of elements such as Fe, Zn, Bi or Sb, we opted not to report these here. We refer the reader to the LA-ICP-MS results for more reliable analyses of minor and trace elements.

Id	Manufacturer/model	Tube	Method	Voltage (kV)	Current (μA)	Collimator	Spot Ø (mm)
pXRF 2011	Olympus InnovX Delta Premium	Au	Alloy Plus	40	12	No	10
pXRF 2012		Rh			100	Yes	3
pXRF 2013							

Table S1. Technical specifications for the three pXRF instruments employed

		Cu	Ag	Au
A1	pXRF2013	1.2	6.2	92.6
	PIXE	1.0	6.4	92.5
	Nominal	2	6	92
A2	pXRF2013	3.0	22.5	74.5
	PIXE	2.8	22.6	74.5
	Nominal	3	27	70
E1	pXRF2013	0.1	49.8	50.1
	PIXE		49	50.7
	Nominal		50	50
E2	pXRF2013	0.5	44.1	55.4
	PIXE	0.5	43.7	55.6
	Nominal	1	44	55

Table S2. Nominal values, and analytical results for PIXE and pXRF 2013 on reference materials. Note that the reference materials were made by a jeweller but may not exactly match the target composition.

	Cu			Ag					Au		
Reference	pXRF 2011	pXRF 2012	δ relative	pXRF 2011	pXRF 2012	δ relative	pXRF 2011*	δ relative*	pXRF 2011	pXRF 2012	δ relative
O33296	1.6	1.9	14%	16.0	14.8	-8%	15.1	2%	82.4	83.4	1%
O33302	2.3	2.3	2%	25.1	23.6	-6%	23.6	0%	72.7	74.1	2%
O33303	9.6	9.5	-1%	18.2	17.1	-7%	17.1	1%	72.2	73.4	2%
O33293	9.7	10.6	8%	16.4	15.2	-8%	15.5	2%	73.8	74.2	1%
O33297	11.4	11.5	1%	14.3	13.4	-6%	13.4	0%	74.3	75.1	1%
O33292	27.4	28.0	2%	15.4	14.5	-6%	14.4	-1%	57.2	57.4	0%

Table S3. Comparison of analytical results for pXRF 2011 and pXRF 2012 on the same objects, before and after calibration of the pXRF 2011 Ag values (post-correction values marked with an asterisk). All analytical results are averages of three or more measurements, and are arranged by ascending Cu values.*

	Cu			Ag			Au		
Reference	pXRF2013	pXRF2012	δ relative	pXRF2013	pXRF2012	δ relative	pXRF2013	pXRF2012	δ relative
O33284	1.0	1.1	11%	16.7	17.3	3%	82.3	81.6	-1%
O33291	1.8	2.1	12%	15.1	15.0	0%	83.1	82.9	0%
O33290	2.1	2.6	21%	16.3	16.4	1%	81.6	81.0	-1%
O33283	5.4	5.8	7%	14.3	14.2	0%	80.3	79.9	0%
O33280	7.4	7.8	6%	15.8	15.7	-1%	76.9	76.5	-1%

Table S4. Comparison of analytical results for pXRF 2012 and pXRF 2013 on the same objects. All analytical results are averages of three or more measurements, and are arranged by ascending Cu values.

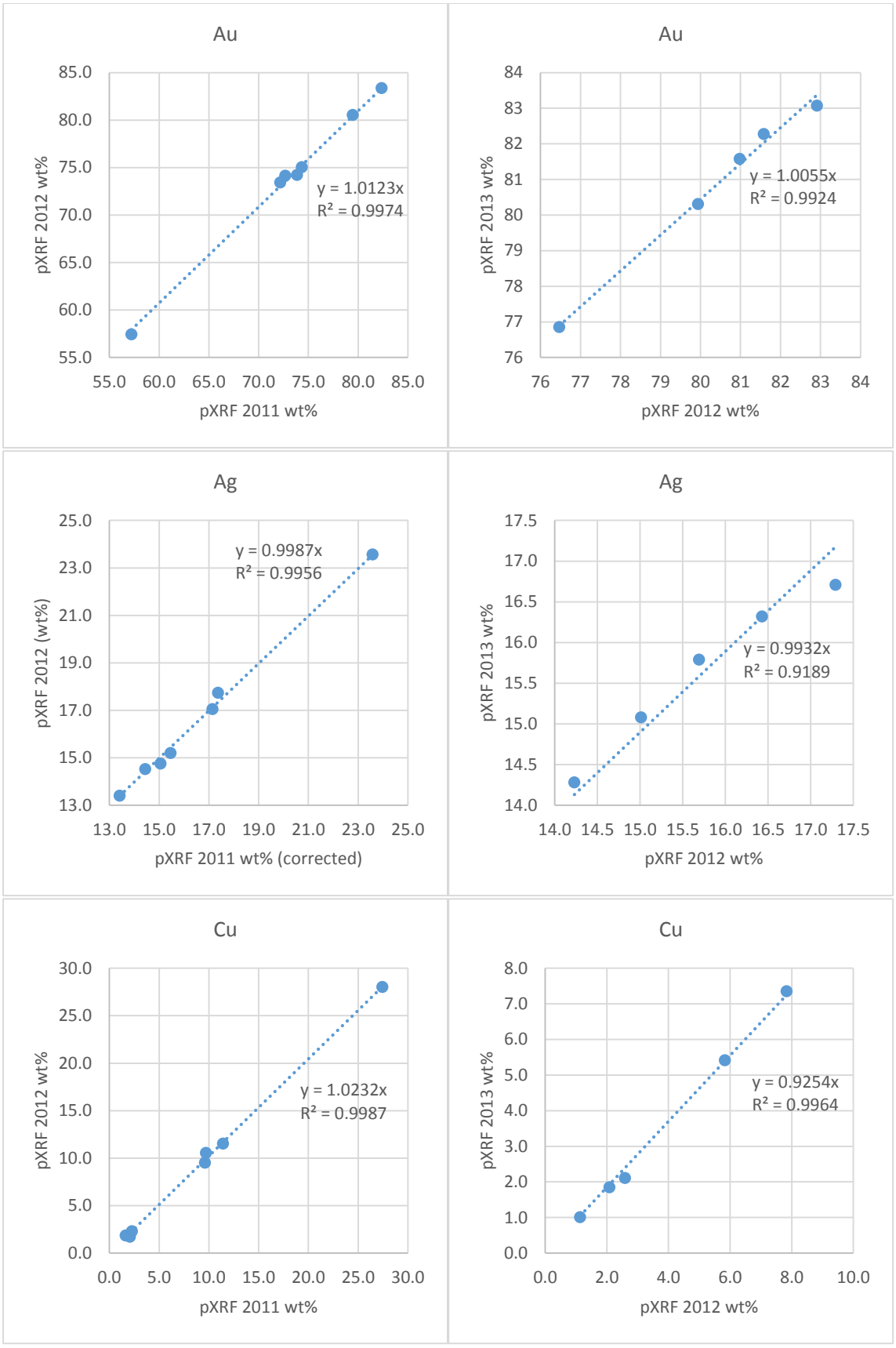

Figure S1. Scatterplots illustrating the comparability between results for pXRF 2011 vs pXRF 2012 (left column) and pXRF 2012 vs pXRF 2013 (right column).

S2. Supplementary information on LA-ICP-MS metal analyses, and comparison with pXRF data.

Analytical protocols for LA-ICP-MS analyses are detailed in the main manuscript text. As noted there, the results reported for Carmen de Carupa, Tocancipá and Suba are from line ablations, whereas those for Tenjo are from spot ablations. Most objects could be analysed only once. A few artefacts, however, were analysed several times, and average values reported in Table 5 of the main manuscript (if only one of the two measurements for a given element was above detection limits, then the average was calculated between the higher value recorded and the nominal quantification limit for that element), while individual results are shown here (Table S5). Some objects were analysed using both spot and line scans in order to assess data reproducibility, and relevant results are also presented in Table S5. Results from both line and spot scans are broadly comparable, especially considering the segregation that exists in these slow-cooled alloys.

				Major			Platinum group elements						Trace elements																
Offering	LA mode	Lab No.	Sample	Cu	Ag	Au	Ru	Rh	Pd	*Os*	Ir	Pt	Ti	Cr	Mn	Fe	Co	Ni	Zn	As	Se	Cd	Sn	Sb	Te	Hg	Tl	Pb	Bi
				%	*%*	*%*	*ppm*	*ppm*	*ppm*	*ppm*	*ppm*	*ppm*	*ppm*	*ppm*	*ppm*	*ppm*	*ppm*	*ppm*	*ppm*	*ppm*	*ppm*	*ppm*	*ppm*	*ppm*	*ppm*	*ppm*	*ppm*	*ppm*	*ppm*
			σ%	*6*	*3*	*3*	*7*	*9*	*5*		*6*	*6*	*6*	*7*	*4*	*5*	*4*	*4*	*6*	*7*	*4*	*4*	*4*	*4*	*13*	*14*		*3*	*12*
			LOQ (ppm)	*100*	*100*	*200*	*0.2*	*0.1*	*1*	*0.2*	*0.1*	*2*	*1*	*2*	*2*	*10*	*2*	*5*	*3*	*10*	*10*	*2*	*5*	*1*	*3*	*5*	*0.5*	*5*	*2*
Carupa	Line	MA-113977	33878	43	8	49	0.54	0.24	2.5	<d.l.	0.13	16	80	20	3	300	<d.l.	18	90	<d.l.	<d.l.	<d.l.	7	2.4	<d.l.	90	<d.l.	12	<d.l.
Carupa	Line	MA-113977	33878	44	10	45	0.68	0.22	1.3	<d.l.	<d.l.	14	40	13	<d.l.	150	<d.l.	18	40	<d.l.	12	<d.l.	8	2.2	<d.l.	100	<d.l.	9	<d.l.
Carupa	Line	MA-113979	33880	39	12	49	0.58	0.21	3.4	*<d.l.*	<d.l.	11	700	40	5	1000	<d.l.	30	140	<d.l.	13	2.5	16	3.0	<d.l.	80	<d.l.	50	20
Carupa	Line	MA-113979	33880	49	8	43	0.64	0.30	<d.l.	*<d.l.*	<d.l.	21	30	20	2	200	<d.l.	<d.l.	70	<d.l.	13	<d.l.	6	1.9	<d.l.	200	<d.l.	12	10
Suba	Line	MA-113974	33303	8	20	72	<d.l.	2.4	7.6	*<d.l.*	<d.l.	140	<d.l.	<d.l.	3	30	<d.l.	<d.l.	20	<d.l.	<d.l.	<d.l.	<d.l.	<d.l.	<d.l.	2000	<d.l.	<d.l.	<d.l.
Suba	Spot	MA-113974	33303	7	18	75	<d.l.	0.81	3.6	*<d.l.*	<d.l.	73	<d.l.	<d.l.	3	30	<d.l.	<d.l.	20	<d.l.	<d.l.	<d.l.	<d.l.	<d.l.	<d.l.	400	<d.l.	<d.l.	<d.l.
Tenjo	Line	MA-113976	33812	20	10	70	0.30	0.31	3.9	*<d.l.*	<d.l.	34	30	<d.l.	4	130	<d.l.	<d.l.	60	<d.l.	<d.l.	<d.l.	<d.l.	1.0	<d.l.	300	<d.l.	5	<d.l.
Tenjo	Line	MA-113976	33812	20	10	70	0.26	0.28	3.1	*<d.l.*	<d.l.	31	5	<d.l.	4	90	<d.l.	<d.l.	50	<d.l.	<d.l.	<d.l.	<d.l.	1.1	<d.l.	300	<d.l.	<d.l.	<d.l.
Tenjo	Spot	MA-113976	33812	24	12	64	0.23	0.32	4.1	*<d.l.*	<d.l.	27	*<d.l.*	6	3	30	0.09	*<d.l.*	80	<d.l.	5	<d.l.	<d.l.	1.9	<d.l.	50	<d.l.	10	<d.l.

Table S5. A comparison of repeat LA-ICP-MS analyses on several objects, using line and spot ablations. LOQ=limit of quantification; <d.l.=below detection limits.

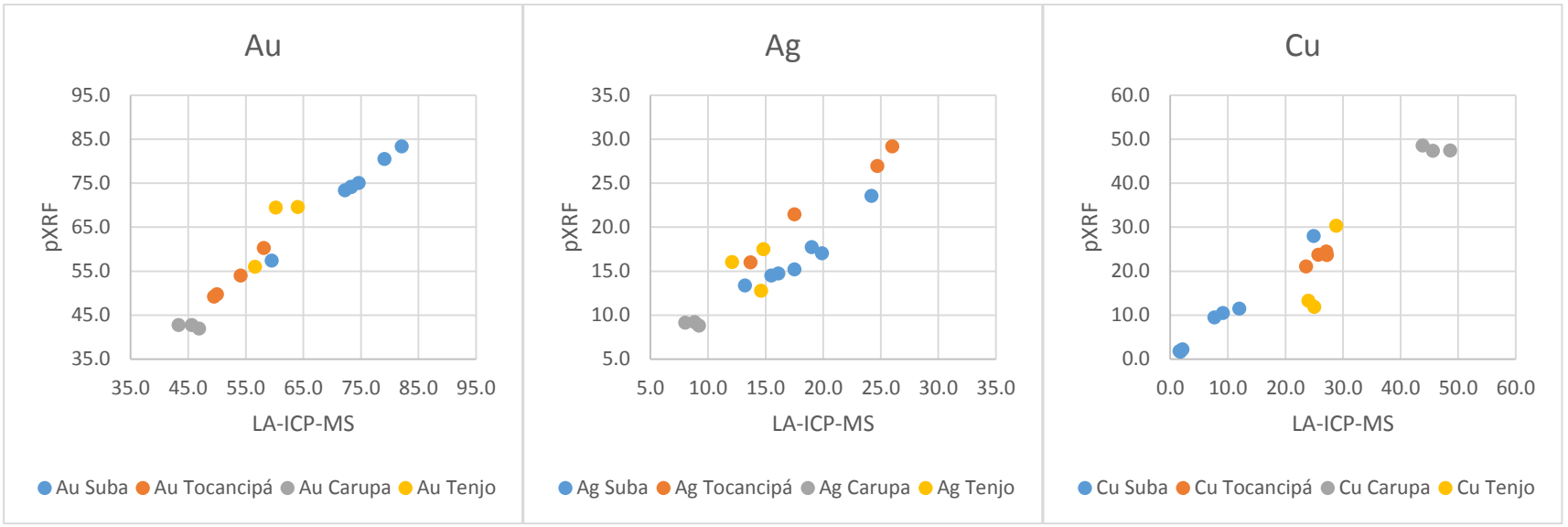

Figure S2. Scatterplots showing a comparison between pXRF and LA-ICP-MS results for the same artefacts. As explained in the main manuscript text, the divergence between some of the results may be explained because of the considerable segregation within the alloys, and the small volumes analysed by the LA-ICP-MS.

S3. Supplementary information on LA-ICP-MS analysis of glass fragment from Tocancipá

Eight small glass fragments (V00017), mostly translucent blue-green in colour and rod-like in shape were recovered with the Tocancipá offering (Figure S3). One of them was subjected to LA-ICP-MS analysis. The analyses were carried out by Matthew Phelps at the IRAMAT Centre Ernest Babelon at Orleans, France. The instrument employed is a Thermo Fisher Scientific Element XR with muticollector, and the laser is a 193nm ArF excimer laser Resolution M50e, operating at an energy of 4mJ and set to 7Hz. This laser uses He (0.6 l/min) and Ar (1.2 l/min) to flush out the system.

Calibration of the instrument used reference materials Nist 610, Corning B, C and D, and APL1 (in-house standard for trace elements). Nist 612 and Corning A are analysed to monitor performance but were not used in the calibration. Blanks are run between standards and every 10-15 analyses to record background levels, which are subtracted from the results.

Three spots were analysed on the sample, each 100µm in diameter, with 20s of pre-ablation and 50s of signal acquisition. Quantification was based on the method described by Gratuze (1999). The results are presented in Table S6.

Figure S3. Glass fragments recovered with the Tocancipá offering. The longest fragment is c. 1 cm in length.

(wt%)	Na2O	Mg O	Al_2O_3	SiO2	P2O5	Cl	K2O	CaO	Mn O	TiO2	Fe2O3
1	0.42	3.05	2.36	60.72	2.17	0.09	6.73	21.65	1.43	0.13	0.68
2	0.43	3.26	2.53	59.60	2.07	0.10	6.67	22.28	1.60	0.13	0.72
3	0.44	3.25	2.51	59.55	2.10	0.10	6.66	22.35	1.61	0.13	0.72

(ppm)	PbO	Li2O	B2O3	V2 O5	Cr2O3	CoO	NiO	CuO	ZnO	GaO	As2O3	Rb2O
1	14	14	537	16	18	220	93	75	192	4	556	150
2	16	11	593	15	19	261	112	83	208	5	589	154
3	17	11	597	16	19	258	113	85	214	5	599	153

(ppm)	SrO	Y2O3	ZrO2	Nb2O3	MoO	SnO2	BaO	La2O3	CeO2	Nd2O3	HfO2	Bi
1	753	6	147	3	4	7	2690	9	18	7	3	54
2	772	6	141	3	4	6	2853	9	16	6	3	66
3	765	6	138	3	4	7	2825	9	16	6	3	66

Table S6. Results of three chemical analyses of glass sample V00017 by LA-ICP-MS, including all elements quantified in concentrations higher than 2ppm.

Reference

Gratuze, B. 1999. Obsidian characterization by laser ablation ICP-MS and its application to prehistoric trade in the Mediterranean and the Near East: sources and distribution of obsidian within the Aegean and Anatolia. *Journal of Archaeological Science*, 26, 869-881.

S4. Supplementary information on the Suba offering. Object descriptions

		Main character/item depicted												Attributes												
	Artisan	Bird figure	Snail figure	Feline figure	Feline skin figure	Spear thrower	Staff with birds	Basket?	Container	Tejuelo	Male	Female	Cot with baby	With dart thrower	With brids / staff with birds	With shield	With crown with rhomboid openwork	With plain crown	With hat	With necklace and pendant	With pouch	With baby	With necklace and spiral ornament	With necklace/ruff	With annular nosering	With necklace with circular beads
33278	2										x			x		x	x									
33279	2										x			x	x	x	x							x		
33280	?										x				x		x			x						
33281	2										x			x			x									
33282	1										x			x			x				x		x	x	x	
33283	2										x			x		x		x								
33284	2										x			x		x		x								
33285	2										x			x		x	x									
33286	?										x				x			x		x						
33287	?											x							x								x
33288	1										x			x	x		x			x	x		x			
33289	?								x		x				x		x						x			
33290	2?										x															
33291	2												x													
33292	1										x			x	x		x			x						
33293	1										x						x									
33294	1											x							x			x				
33295	1																	x								

		Main character/item depicted												Attributes												
	Artisan	Bird figure	Snail figure	Feline figure	Feline skin figure	Spear thrower	Staff with birds	Basket?	Container	Tejuelo	Male	Female	Cot with baby	With dart thrower	With brids / staff with birds	With shield	With crown with rhomboid openwork	With plain crown	With hat	With necklace and pendant	With pouch	With baby	With necklace and spiral ornament	With necklace/ruff	With annular nosering	With necklace with circular beads
33296	1											x							x			x	x			
33297	1										x				x		x				x					
33298	1										x															
33299	1?				x																					
33300	1												x													
33301	2?												x													
33302	1												x													
33303	1												x													
33304	1?						x																			
33305	1?	x																								
33306	1?							x																		
33307	1					x																				
33308	1?			x																						
33309	1?	x																								
33310	?									x																
33311	1?		x																							
Total	34	2	1	1	1	1	1	1	1	1	17	3	5	9	8	5	11	4	3	4	3	2	4	2	1	1

S5. Supplementary information on principal component analysis (PCA)

Principal component analyses of LA-ICP-MS results for all the offerings together were performed on the normalised subcomposition of Ru, Rh, Pd, Ir, Pt, Ti, Cr, Mn, Fe, Ni, Zn, Sn, Sb, Hg, Pb and Bi. Only the Tocancipá spherule O33898e was excluded as an outlier, to maximise separation of the other samples. Lost values were replaced with the quantification limit for the given element. The other trace elements were not included in the PCA because there were too many values below quantification limits. We assessed correlation matrices for full and single-site sets of the data. Having observed that there were no meaningful correlations between major and trace elements in the dataset (see main text for explanation), we chose to use a normalised subcomposition to identify any underlying structure created by trace element patterns (as opposed to the main alloying constituents). A plot of the relevant scores on the first three principal components is shown in Figure 19 of the article, while relevant statistics are reported here in table form (Table S7).

Component	Initial Eigenvalues			Extraction Sums of Squared Loadings		
	Total	% of Variance	Cumulative %	Total	% of Variance	Cumulative %
1	4.661	29.128	29.128	4.661	29.128	29.128
2	3.402	21.265	50.394	3.402	21.265	50.394
3	2.558	15.989	66.382	2.558	15.989	66.382
4	1.422	8.885	75.267	1.422	8.885	75.267
5	1.357	8.483	83.750	1.357	8.483	83.750

	PC1	PC2	PC3	PC4	PC5
Ru	.915	.014	-.038	.037	.016
Rh	.740	-.467	.278	-.154	.105
Pd	.878	-.241	.297	.011	.120
Ir	.541	.480	.520	.090	-.012
Pt	.762	-.472	.371	-.073	.079
Ti	.387	.344	-.601	-.336	-.202
Cr	.498	.238	-.680	.000	-.290
Mn	.621	.021	.165	.389	.193
Fe	.347	.394	-.640	.169	.429
Ni	.731	.392	-.209	.050	-.400
Zn	-.158	.561	.417	.225	-.419
Sn	-.162	.322	.507	.394	-.316
Sb	-.176	.239	-.213	.683	.526
Hg	-.274	-.900	-.070	-.073	.009
Pb	-.188	.691	.369	-.452	.233
Bi	.034	.653	.249	-.453	.461

Table S7. Principal component analysis of LA-ICP-MS results for the four offerings. Top, total variance explained by the five principal components with eigenvalues higher than 1. Bottom, component matrix. See Figure 19 for a plot of the samples on PC1 and PC2.

An additional PCA was performed with major and minor elements from the LA-ICP-MS of all the artefacts in the Tocancipá offering analysed, including the spherule excluded in the previous PCA. This allowed us to confirm the presence of chemical subgroups corresponding with typological categories, as suggested by pXRF.

Component	Initial Eigenvalues			Extraction Sums of Squared Loadings		
	Total	% of Variance	Cumulative %	Total	% of Variance	Cumulative %
1	7.928	44.047	44.047	7.928	44.047	44.047
2	3.392	18.842	62.889	3.392	18.842	62.889
3	2.604	14.465	77.354	2.604	14.465	77.354
4	2.051	11.394	88.748	2.051	11.394	88.748
5	1.011	5.618	94.366	1.011	5.618	94.366

	PC1	PC2	PC3	PC4	PC5
Cu	.050	-.979	-.106	.076	-.124
Ag	-.223	.360	-.757	.360	.157
Au	-.061	.718	.594	-.273	-.005
Ru	.086	-.452	.615	.474	.014
Rh	.960	.062	.157	.138	-.079
Pd	.808	-.070	.348	.324	-.154
Ir	.942	-.068	-.083	-.101	.009
Pt	.963	.042	.110	.118	-.105
Ti	.388	.186	-.591	.323	-.458
Cr	-.130	.519	.405	-.680	-.100
Mn	.000	.038	.725	.650	.203
Fe	.066	.630	-.211	.439	.587
Ni	.969	-.033	-.064	-.182	.115
Zn	-.082	-.774	-.023	-.349	.453
Sn	.960	.209	-.048	-.104	.019
Sb	.922	.297	-.109	-.093	.155
Pb	.781	-.364	-.139	-.333	.285
Bi	.990	-.035	-.029	-.042	.002

Table S8. Principal component analysis of LA-ICP-MS results for the Tocancipá offering. Top, total variance explained by the five principal components with eigenvalues higher than 1. Bottom, component matrix. See Figure S4 for a plot of the samples on PC1 and PC2.

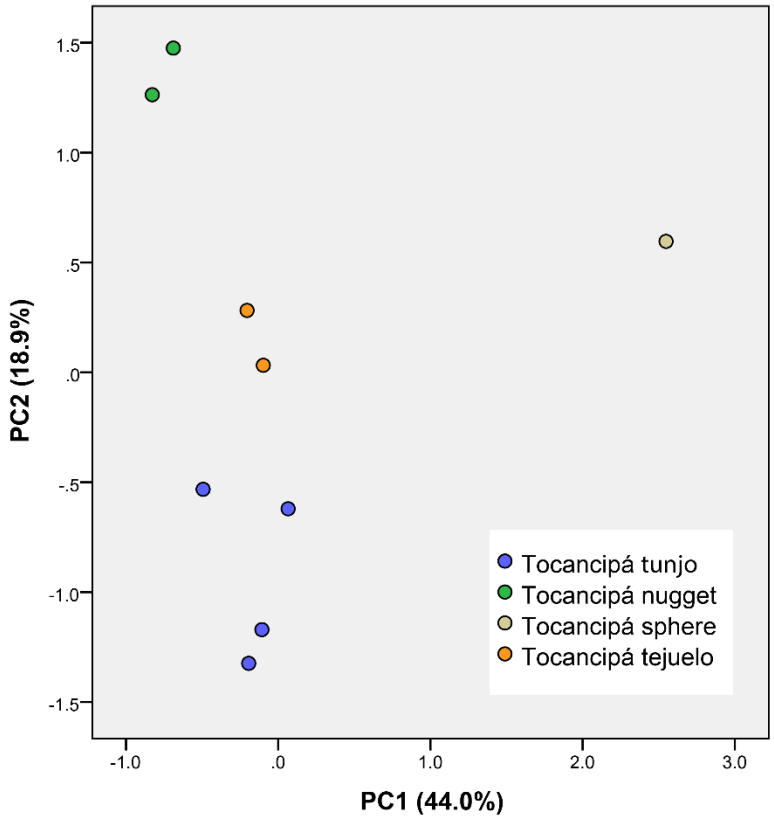

Figure S4. Plot of the loading scores for the Tocancipá artefacts on the first two principal components after PCA of the LA-ICP-MS data.